



Exploring topological materials for hydrogen evolution reaction: insights from density functional theory

Jing Yang¹, Yaze Wu¹, Zhigen Yu¹, Antonio Politano², Danil Bukhvalov³, Anna Cupolillo⁴, Haisong Feng^{1,5,*}, Xin Zhang^{5,*}, Yong-Wei Zhang^{1,*}

Keywords:

Topological materials, HER, density functional theory, catalysts

Citation: Yang, J.; Wu, Y.; Yu, Z.; Politano, A.; Bukhvalov, D.; Cupolillo, A.; Feng, H.; Zhang, X.; Zhang, Y. W. Exploring topological materials for hydrogen evolution reaction: insights from density functional theory. *Energy Mater.* 2026, 6, 600029.
<https://dx.doi.org/10.20517/energymater.2025.184>

Received: 31 Oct 2025

First Decision: 11 Dec 2025

Revised: 15 Jan 2026

Accepted: 27 Jan 2026

Published: 24 Mar 2026

Academic Editor:

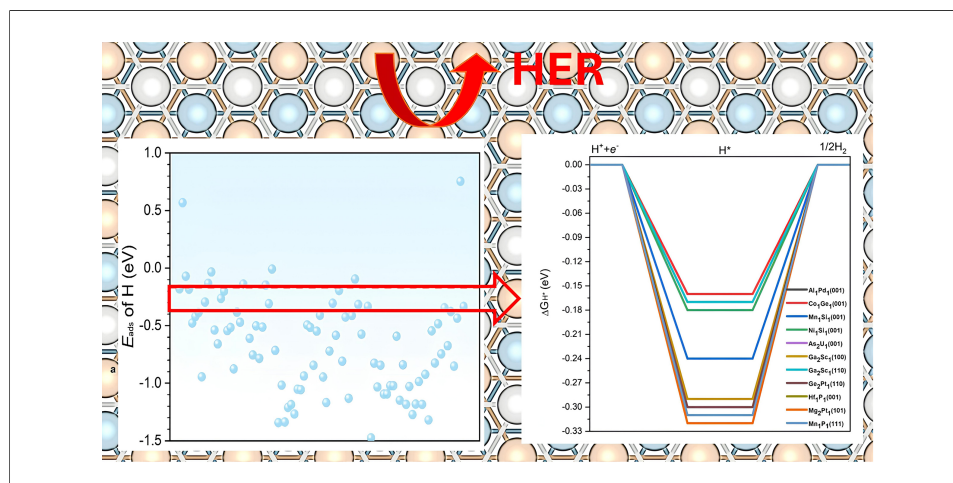
Yizhong Huang

Copy Editor:

Ping Zhang

Production Editor:

Ping Zhang



Abstract

Hydrogen energy technologies offer a transformative shift toward reducing reliance on fossil fuels and creating a sustainable, low-carbon future. In this shift, topological materials, known for their strong electron interactions and unique physical properties, present promising opportunities in electrocatalysis. In this study, we performed a systematic density functional theory analysis of over 100 topological materials and examined more than 1,000 adsorption sites. Our findings reveal that topological materials possess abundant and diverse active sites, resulting in a wide range of hydrogen adsorption energies ranging from -1.5 eV to 0 eV. To identify the most promising catalysts for hydrogen evolution reaction (HER) in acidic media, we focused on the topological materials with hydrogen adsorption energies within -0.27 ± 0.1 eV. The Gibbs free energy of

¹Institute of High Performance Computing (IHPC), Agency for Science, Technology and Research (A*STAR), Singapore 138632, Singapore.

²Department of Physical and Chemical Sciences, University of L'Aquila, L'Aquila 67100, Italy.

³College of Science & Institute of Materials Physics and Chemistry, Nanjing Forestry University, Nanjing 210037, Jiangsu, China.

⁴Department of Physics, University of Calabria, Rende 87036, Italy.

⁵State Key Laboratory of Chemical Resource Engineering, Beijing Advanced Innovation Center for Soft Matter Science and Engineering, Beijing University of Chemical Technology, Beijing 100029, China.

***Correspondence to:** Dr. Haisong Feng, Institute of High Performance Computing (IHPC), Agency for Science, Technology and Research (A*STAR), Singapore 138632, Singapore; State Key Laboratory of Chemical Resource Engineering, Beijing Advanced Innovation Center for Soft Matter Science and Engineering, Beijing University of Chemical Technology, Beijing 100029, China. E-mail: fenghaisong@buct.edu.cn; Prof. Xin Zhang, State Key Laboratory of Chemical Resource Engineering, Beijing Advanced Innovation Center for Soft Matter Science and Engineering, Beijing University of Chemical Technology, Beijing 100029, China. E-mail: zhangxin@mail.buct.edu.cn; Prof. Yong-Wei Zhang, Institute of High Performance Computing (IHPC), Agency for Science, Technology and Research (A*STAR), Singapore 138632, Singapore. E-mail: zhangyw@ihpc.a-star.edu.sg

hydrogen adsorption (ΔG_{H^*}) was evaluated for the HER. All selected materials showed ΔG_{H^*} values between -0.31 and -0.16 eV. Based on these results, 11 promising candidates were identified with high potential for efficient HER activity. Our study establishes fundamental structure-property-activity relationships that can serve as a reliable dataset for further machine-learning studies, while also providing valuable insights and design guidelines for the continued exploration of topological materials as high-performance HER catalysts.

INTRODUCTION

Hydrogen energy technologies have been recognized as a promising candidate to reduce dependence on fossil fuels and meet future energy demands^[1,2]. Currently, fossil fuels, including natural gas, coal, and oil, account for approximately 80% of the world's energy consumption^[3]. The combustion of fossil fuels releases large amounts of greenhouse gases, leading to more severe weather events, rising sea levels, and declining biodiversity. Additionally, it also fuels geopolitical conflicts and energy security concerns due to the unequal distribution of reserves^[4,5]. In response to these growing environmental concerns and energy security challenges, hydrogen has the potential to drive the global transition toward a more sustainable, low-carbon future^[6].

The development of highly efficient, selective, stable, and cost-effective catalysts for the water-splitting process is the crucial step toward a thriving hydrogen economy. Utilizing electrocatalysts along with electricity from renewable sources for the hydrogen evolution reaction (HER) is one of the most promising approaches. Platinum-group metals, especially platinum and its alloys, have emerged as the most effective electrocatalysts for this process^[7-9]. Among them, the ultralow-Pt-loading electrocatalysts, which can reach the balance of low cost and high HER performance, have attracted much attention. Chen *et al.* demonstrated that anchoring platinum clusters onto two-dimensional fullerene nanosheets (PtC₆₀) significantly boosts platinum's activity for the alkaline HER. This PtC₆₀ composite shows 12 times higher intrinsic activity compared to the traditional Pt/C catalyst in alkaline conditions^[10]. Smiljanić *et al.* reported a novel composite catalyst consisting of Pt nanoparticles supported on TiON_x (Pt/TiON_x), which outperformed the benchmark Pt/C catalyst regarding both HER activity and stability in acid electrolytes^[11]. Other transition metals (Co, Fe, Mo, Ni, *etc.*) have also been explored as effective electrocatalysts for HER in recent years to confront the scarcity and high cost of Pt^[12-15]. At the same time, single-atom catalysts (SACs) are receiving increasing attention due to the maximized atom utilization efficiency arising from their abundant active sites^[16-18]. Yet, the search for electrocatalysts that simultaneously combine high activity, selectivity, stability, and cost-effectiveness remains ongoing.

Topological materials, known for their strong electron interactions and distinctive physical properties, provide exciting new opportunities in the field of electrocatalysis^[19,20]. With their unique surface states and exceptional charge mobility, they emerge as highly effective electrocatalysts capable of addressing the limitations of current hydrogen production technologies^[21]. Qu *et al.* found that Bi₂Te₃ topological insulator thin films, when having partially oxidized surfaces or tellurium vacancies, show high activity for HER, with a current density reaching up to $1.74 \mu\text{A cm}^{-2}$ for a 48 nm Bi₂Te₃ thin film^[22]. Through first-principles calculations, Li *et al.* reported a new topological nodal line semimetal, namely the TiSi-type family, which exhibits a closed Dirac nodal line arising from linear band crossings in the $k_y = 0$ plane. The hydrogen adsorbed state on the corresponding surface yields ΔG_{H^*} (ΔG_{H^*} represents the Gibbs free energy of hydrogen adsorption, where * denotes an active site on the catalyst surface) close to zero, indicating near-optimal activity for HER^[23]. Our group has explored the topological nodal-line semimetal AuSn₄, discovering that oxidized AuSn₄ can be an effective catalyst for HER in alkaline media^[24].

Despite numerous efforts, the search for the optimal electrocatalyst for HER remains ongoing; the structure-property-activity relationships of topological materials are still missing. In this work, we conduct density functional theory (DFT) calculations to systematically screen topological materials, aiming to identify high-performance topological material catalysts specifically suited for HER. Our study screens 1,000 sites across nearly 100 surfaces of topological materials and identifies 11 topological materials promising as superior electrocatalysts for HER. Our study not only helps better understand topological materials and their relationship to HER but also provides guidance for future research in material synthesis and electrochemistry toward developing more effective HER catalysts.

CALCULATION METHOD

The DFT calculations were carried out by using the plane-wave-based Vienna Ab initio Simulation Package (VASP 5.4.1)^[25,26]. The exchange-correlation interactions were modeled using the Perdew-Burke-Ernzerhof (PBE) functional within the framework of the generalized gradient approximation (GGA)^[27]. This functional has been widely demonstrated to provide a reliable description of the electronic structure and energetics of solid-state and surface systems. The interactions between core and electrons were described with the projector augmented wave (PAW) method^[28-30], enabling an accurate yet computationally efficient representation of the ionic cores. All atomic structures were fully optimized prior to property calculations, with both atomic positions allowed to relax until the residual forces on each atom were smaller than 0.02 eV Å⁻¹. The electronic self-consistent field calculations were considered converged when the total energy difference between successive ionic steps was less than 10⁻⁶ eV, ensuring well-converged total energies and reliable adsorption energetics. For Brillouin zone integration, a 3 × 3 × 1 k-point mesh was employed using the Monkhorst-Pack scheme, which is appropriate for slab and surface models and provides a good balance between accuracy and computational cost. To properly capture weak long-range interactions that are not adequately described by conventional GGA functionals, van der Waals corrections were included using Grimme's semi-empirical density functional theory with D3 dispersion correction (DFT-D3) method^[31]. This correction is particularly important for surface and low-dimensional systems, where dispersion interactions can play a significant role in adsorption behavior. The combination of these computational settings ensures a consistent and reliable evaluation of the structural and energetic properties of the investigated systems. The adsorption energies (E_{ads}) of the proton were calculated as $E_{\text{ads}} = E_{\text{total}} - E_{\text{surf}} - E_{\text{H}}$, where E_{total} , E_{surf} , and E_{H} represent the energies of optimized adsorption configurations, empty model surface, and half of the H₂ molecule, respectively. The HER performance was evaluated by the ΔG_{H^*} of the reaction [ΔG_{H^*} was calculated using $\Delta G_{\text{H}^*} = \Delta E_{\text{H}^*} + \Delta \text{ZPE} - T\Delta S$, where ΔE_{H^*} is the energy difference of E_{ads} , and ΔZPE and $T\Delta S$ (where T is the temperature and ΔS is the entropy change) are the changes of zero-point energy and entropy of H⁺ adsorption, respectively]. In this study, $T\Delta S$ and ΔZPE were obtained by following the scheme proposed by Nørskov *et al.*^[32]. Numerous experimental and theoretical studies have established a strong correlation between ΔG_{H^*} and HER activity^[23], demonstrating that ΔG_{H^*} serves as a robust and physically meaningful descriptor for HER performance. Accordingly, this descriptor is also employed in the present study. According to established literature correlations, the optimal ΔG_{H^*} corresponds to a target adsorption energy of -0.27 eV^[31].

RESULTS AND DISCUSSION

Adsorption sites

The intricate surface structure of topological materials provides rich reaction sites, making these materials promising candidates in the field of catalysis. Given that low-index crystal facets are more energetically favorable and thus more amenable to synthesis, this study focuses on all the low-index crystal facets, including (001), (100), (101), (110), and (111) surfaces [Figure 1]. These facets differ markedly in their atomic arrangements, surface atom coordination numbers, and bonding environments. Such variations lead to

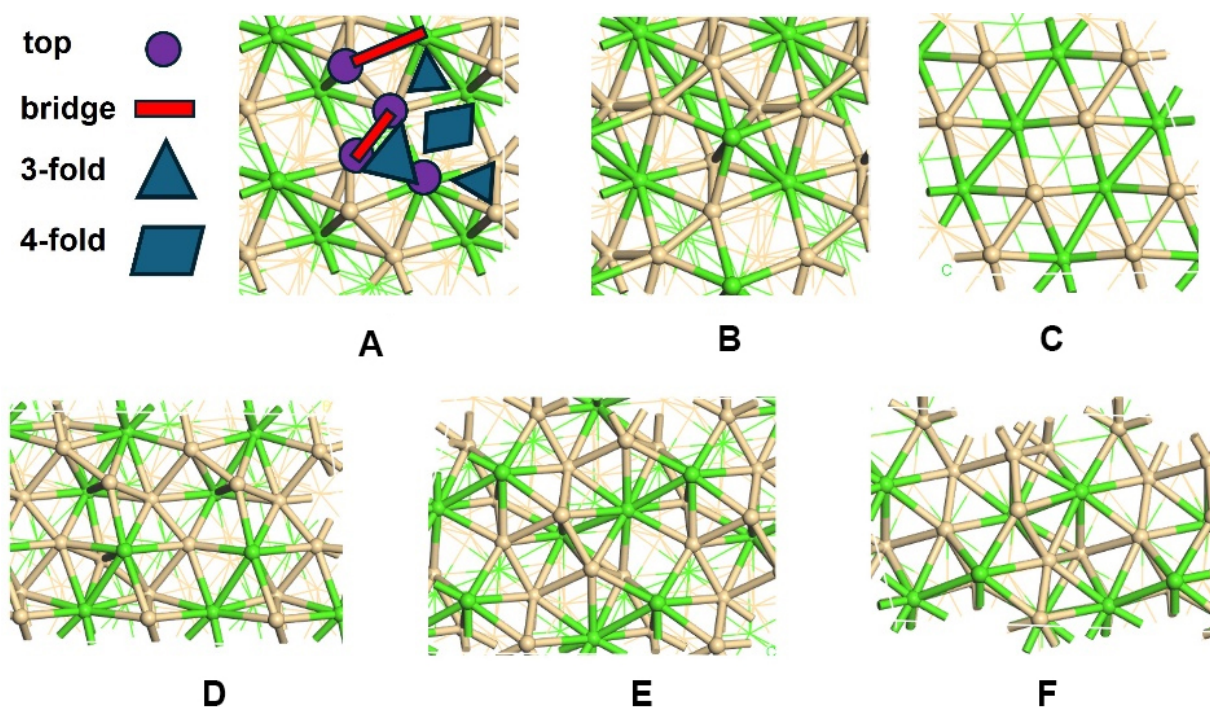


Figure 1. All the possible low-index facets and adsorption sites studied in this work. (A and B) Cr,Ce, (001) surface with Cr and Ce termination, respectively; (C-F): (100), (101), (110) and (111) surfaces. Green and ochre spheres represent Cr and Ce atoms, respectively. The different adsorption sites: top, bridge, 3-fold and 4-fold hollow sites are illustrated in Figure 1A.

different local electronic structures and adsorption geometries, thereby creating diverse reaction conditions across the surface, which may result in more active sites available for enhanced activities.

Distinct surface terminations give rise to a variety of adsorption sites, each of which can have a significant impact on HER performance. Therefore, it is essential to examine all possible adsorption sites to gain a complete and accurate understanding of the catalytic performance. To ensure a systematic and thorough study, our investigation carefully examines all potential reaction sites on each surface, encompassing metal, non-metal, and mixed terminations. For every termination, we consider all possible adsorption positions, including top sites located directly above individual surface atoms, bridge sites between two adjacent atoms, and hollow sites at the center of three or more neighboring atoms [Figure 1A]. A comprehensive analysis of catalytic performance at all the possible sites was conducted to identify the most stable adsorption site.

Adsorption energies

Adsorption plays a crucial role in surface reactions, as an ideal catalyst should have an intermediate binding affinity for reactants. The adsorption needs to be strong enough to facilitate the reaction but not so strong that it prevents the easy desorption of the products^[33]. The adsorption energy of hydrogen on topological material varies in a wide range, as summarized in Table 1. As expected, the topological materials give abundant adsorption sites, leading to a wide range of adsorption energies for hydrogen. The most favorable adsorption sites also vary among different materials. On Al₁Pt₁ (001), the hydrogen prefers the Pt-top site, with a hydrogen adsorption energy (E_{ads}) calculated to be 0.57 eV, indicating that hydrogen adsorption on Al₁Pt₁ is endothermic and not energetically favorable. As a result, Al₁Pt₁ (001) is expected to be inactive for HER because hydrogen adsorption is not energetically favorable, making subsequent reactions difficult. In contrast, on the Al₁Au₁ (110) surface, the hydrogen prefers the Al-top side, with an E_{ads} calculated to be -2.22 eV, indicating a strong binding between hydrogen and Al₁Au₁ (110) surface. However, such a strong binding corresponds to the high energy cost of release of hydrogen from the substrate. Thus, Al₁Au₁ (110) is

Table 1. Hydrogen adsorption energy (E_{ads} in eV) at the most favorable adsorption site for each material and surface termination; top, bridge, and hollow sites denoted by _t, _b, and _h, respectively

Material	E_{ads}	Sites	Material	E_{ads}	Sites	Material	E_{ads}	Sites
Al ₁ Pd ₁ _001	-0.18	Al-Pd-bri	Al ₁ La ₁ _111	-0.88	Al-La_b	C ₁ Hf ₁ _111	-2.16	Hf-Hf_h
Al ₁ Pt ₁ _001	0.57	Pt-top	Ba ₁ Sn ₁ _111	-0.38	BaBaBa_h	C ₁ Ti ₂ _101	-1.21	Ti3_h
Au ₁ Be ₁ _001	-0.07	Au-Be_b	Ba ₂ Zn ₁ _111	-0.47	ZnZnZn_h	C ₁ Ti ₂ _110	-1.19	Ti-Ti_b
Co ₁ Ge ₁ _001	-0.18	Co_t	Bi ₁ Li ₁ _111	-0.14	Bi-Li_b	C ₁ Ti ₂ _111	-1.27	Ti3_h
Co ₁ Si ₁ _001	-0.48	Co-Co_b	Al ₁ Au ₁ _110	-2.22	Al_t	C ₁ V ₂ _101	-1.05	V-V_b
Cr ₁ Ge ₁ _001	-0.42	Cr-Cr_b	Al ₁ La ₁ _110	-0.61	Al-La_b	Cu ₁ Ti ₂ _001	-1.06	Cu3_h
Cr ₁ Si ₁ _001	-0.39	Cr-Cr_b	Al ₁ Sc ₁ _110	-0.75	Al-Al-Sc_h	Cu ₁ Ti ₂ _111	-0.94	CuTi_h
Fe ₁ Pd ₁ _001	-0.94	Fe_t	Al ₁ La ₁ _001	-0.50	La-La_b	Fe ₁ Pt ₁ _100	-0.49	Pt_t
Ga ₁ Pt ₁ _001	-0.29	Pt_t	Al ₁ Pt ₂ _001	-0.78	Al_t	Fe ₁ Pt ₁ _101	-0.52	Fe-Fe-Pt_h
Ge ₁ Mn ₁ _001	-0.13	Mn-Mn_b	Al ₁ Sc ₁ _001 ²	-0.51	AlAl_b	Fe ₁ Pt ₁ _110	-4.20	NA
Ge ₁ Rh ₁ _001	-0.03	Rh_t	As ₁ Rh ₁ _001	-0.15	Rh-Rh_b	Fe ₁ Pt ₁ _111	-2.45	Fe_t
Hf ₁ Sb ₁ _001	-0.54	Hf-Hf_b	As ₂ U ₁ _001	-0.31	As_t	Ga ₁ Mn ₁ _001	-0.84	Ga-Mn_b
Hf ₁ Sn ₁ _001	-0.66	Hf-Hf_b	C ₁ Ni ₁ _001	-0.01	Ni-Ni_h	Ga ₁ Sc ₁ _001	-0.55	Ga_t
Mn ₁ Si ₁ _001	-0.26	Mn-Si_b	C ₁ W ₁ _001	-0.71	W-W_h	Ga ₁ Sc ₁ _100	-0.41	Ga-Sc_b
Ni ₁ Si ₁ _001	-0.20	Si_t	C ₁ Zr ₁ _001	-1.34	Zr-Zr_h	Ga ₁ Sc ₁ _101	-0.95	Ga-Sc_b
Re ₁ Si ₁ _001	-0.54	Re_t	Ce ₁ O ₁ _001	-1.02	Ce-Ce_h	Ga ₁ Sc ₁ _110	-1.17	Ga-Sc_b
Si ₁ V ₁ _001	-0.52	V-V_b	H ₁ V ₁ _001	-1.34	V-V_h	Ga ₁ Sc ₁ _111	-0.72	Sc_t
Ga ₂ Sc ₁ _100	-0.31	Ga-Sc_b	Hf ₁ P ₁ _110	-1.03	Hf_t	Hf ₂ Rh ₁ _100	-0.92	Hf-Rh_b
Ga ₂ Sc ₁ _101	-0.58	Ga_t	Hf ₁ P ₁ _111	-0.84	Hf_t	Hf ₂ Rh ₁ _110	-2.25	HfHfHf_h
Ga ₂ Sc ₁ _110	-0.19	Ga-Ga_b	Hf ₁ Ru ₁ _001	-1.09	Hf-Ru_b	Ir ₁ Ta ₁ _001	-3.40	Ta_t
Ga ₂ Sc ₁ _111	-0.81	Sc_t	Hf ₁ Ru ₁ _100	-1.09	Hf-Hf_b	Ir ₁ Ta ₁ _101	-1.32	Ta_t
Ga ₂ Th ₁ _001	-0.43	Ga_t	Hf ₁ Ru ₁ _101	-1.02	Hf-hf_b	Ir ₁ Ta ₁ _111	-0.55	Ta-Ta_b
Ga ₂ Th ₁ _100	-1.13	GaThTh_h	Hf ₁ Ru ₁ _110	-1.02	Ru_t	Ir1V1_111	-0.82	Ir_t
Ge ₂ Pt ₁ _001	-0.41	Ge-Pt_b	Hf ₁ Ru ₁ _111	-0.59	Ru_t	Mg ₂ Pt ₁ _001	-0.48	Pt_t
Ge ₂ Pt ₁ _100	-0.10	Ge-Pt_b	Hf ₂ Hg ₁ _001	-1.15	Hf-Hf_b	Mg ₂ Pt ₁ _100	-0.75	Mg_t
Ge ₂ Pt ₁ _101	-3.88	Pt_t	Hf ₂ Hg ₁ _100	-0.84	Hg_t	Mg ₂ Pt ₁ _101	-0.34	MgMgMg_h
Ge ₂ Pt ₁ _110	-0.32	Pt_top	Hf ₂ Hg ₁ _101	-1.18	HfHgHg_h	Mg ₂ Pt ₁ _110	-0.67	Mg_t

Ge ₂ Ti ₁ _101	-0.57	GeGeTi_h	Hf ₂ Hg ₁ _110	-1.03	Hf-Hf-Hf_h	Mn ₁ P ₁ _001	-0.38	Mn-Mn_b
Ge ₂ Ti ₁ _110	-1.61	Ti_t	Hf ₂ Hg ₁ _111	-1.27	Hg_t	Mn ₁ P ₁ _100	-0.85	P_t
Hf ₁ P ₁ _001	-0.33	Hf_t	Hf ₂ Ni ₁ _101	-1.18	Hf-Hf-Hf_h	Mn ₁ P ₁ _101	-0.43	MnP_b
Hf ₁ P ₁ _100	-1.47	HfP_b	Hf ₂ Ni ₁ _110	-0.98	Hf-Hf-Hf_h	Mn ₁ P ₁ _110	0.75	MnP_h
Hf ₁ P ₁ _101	-0.83	Hf_t	Hf ₂ Ni ₁ _111	-1.18	Hf-Hf-Hf_h	Mn ₁ P ₁ _111	-0.33	P_t

also expected to be inactive for HER. For Al₁Pd₁(001), hydrogen prefers a Pd top site and the calculated adsorption energy is -0.18 eV. Such an adsorption is moderate, which might be optimal for effective HER. Detailed adsorption properties can be found in [Table 1](#).

Statistical analysis shows that hydrogen adsorption energies on the surfaces of topological materials predominantly fall within -1.5 eV to 0 eV. As a result, we selected candidates whose E_{ads} values satisfy these criteria. This focus was also motivated by the observation that the systems with E_{ads} outside this range tend to bind hydrogen either too weakly or too strongly, making them unsuitable for further consideration. As summarized in [Figure 2](#), the topological materials exhibit a well-distributed range of E_{ads} values, highlighting their potential to provide abundant active sites. In addition, most of the selected topological materials possess a moderate adsorption capacity for hydrogen atoms, making them promising candidates for efficient HER.

Preferred adsorption sites of the selected topological materials

It was reported that optimal activity and selectivity can be achieved when E_{ads} of hydrogen is -0.27 eV^[32,34]. This criterion is based on previous studies showing that adsorption energies close to -0.27 eV typically balance the hydrogen binding strength required for optimal HER activity. Grimme *et al.* demonstrated that adsorption energy near -0.27 eV is often ideal for achieving high HER activity across a variety of catalysts, providing a balance between adsorption and desorption processes^[31]. Similarly, studies by Greeley *et al.* have reinforced that an optimal adsorption range enhances catalytic efficiency and stability^[33]. With this criterion, we have pinpointed 11 distinct surfaces, with each displaying E_{ads} of hydrogen within a 0.1 eV range of the optimal benchmark of -0.27 eV, as shown in [Figure 3](#).

After identifying the promising topological materials for HER, we systematically summarized the detailed atomic structures and adsorption behaviors of their surfaces, as illustrated in [Figure 4](#). Interestingly, the favorable adsorption sites for hydrogen vary depending on both the material and the specific surface facet and can be the top, bridge, and hollow sites. This variation reflects the influence of local atomic arrangements, coordination numbers, and electronic environments on hydrogen binding. For example, hydrogen prefers Al-Pd bridge sites on Al₁Pd₁(001) surface, where it can form optimal interactions with both neighboring atoms simultaneously, with the E_{ads} calculated to be -0.18 eV. In contrast, hydrogen prefers Co-top sites with a slight tilt toward the neighboring Ge atom on the Co₁Ge₁(001) surface, with the E_{ads} calculated to be -0.18 eV. In the case of Ga₂Sc₁, both (100) and (110) serve as favorable hydrogen adsorption sites, but the preferred adsorption configurations differ between the facets. On the (100) surface, hydrogen binds most stably at the Ga-Sc bridge site, whereas on the (110) surface, the Ga-Ga bridge site is favored. The

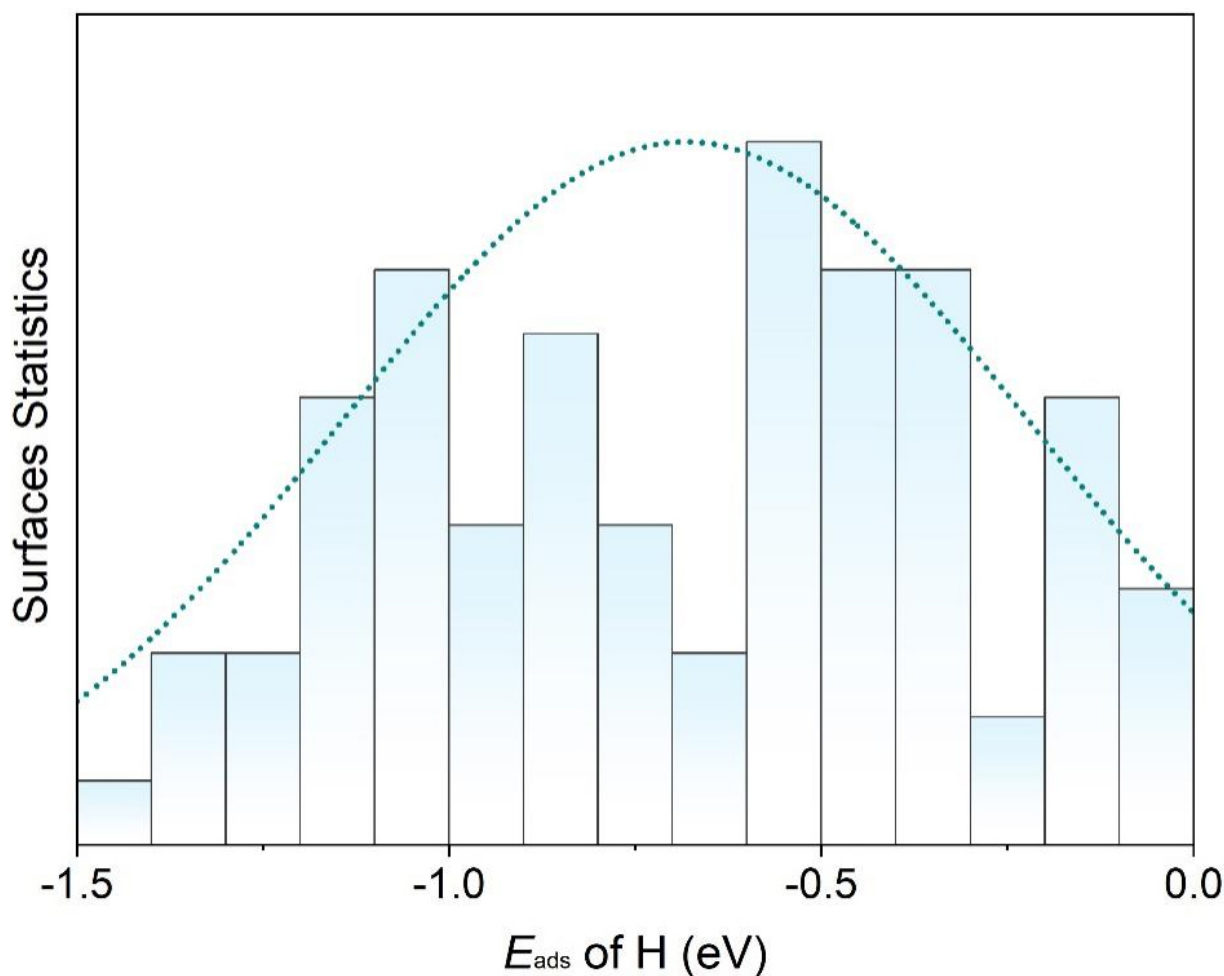


Figure 2. Normalized distribution of E_{ads} (as in Table 1) for hydrogen on various topological materials, showing a well-distributed range and predominantly moderate hydrogen adsorption.

hydrogen adsorption energies on these two sites are calculated to be -0.31 eV and -0.19 eV, respectively. For the case of $\text{Ge}_2\text{Pt}_1(110)$, hydrogen prefers Pt top sites with an E_{ads} of -0.32 eV. These differences of the preferred adsorption sites highlight how subtle variations in surface atomic arrangement and termination can lead to distinct adsorption behaviors. The details of other geometries can be found in Figure 4. Overall, these observations highlight the critical importance of thoroughly examining multiple surfaces and adsorption sites for each material. Meanwhile, as expected, these topological materials offer robust surfaces and adsorption sites, which can accommodate hydrogen with optimal adsorption strength.

Gibbs free energy calculations

The ΔG_{H^+} is a well-accepted descriptor that has been successfully applied to predict HER activities^[35]. Previous studies have established that an ideal ΔG_{H^+} close to zero is a strong indicator of effective HER activity, as it suggests a balanced adsorption and desorption process, which is critical for optimal hydrogen evolution^[31,33]. Focusing on these 11 topological materials, we further calculated the ΔG_{H^+} and the results are summarized in Figure 5. It is seen that the ΔG_{H^+} values range from -0.16 eV to -0.32 eV, suggesting that these surfaces have the potential to function as high-performance catalysts for HER. Among these 11 topological materials, $\text{Al}_1\text{Pd}_1(001)$, $\text{Co}_1\text{Ge}_1(001)$, $\text{Ni}_1\text{Si}_1(001)$ and $\text{Ga}_2\text{Sc}_1(110)$ demonstrate ΔG_{H^+} of -0.16, -0.16, -0.18 and -0.17 eV, respectively. These four candidates are expected to possess the topmost HER performance. Interestingly, Ga_2Sc_1 possesses two active facets, that is, (100) and (110), both of which possess superior HER activity, highlighting its excellent catalytic performance.

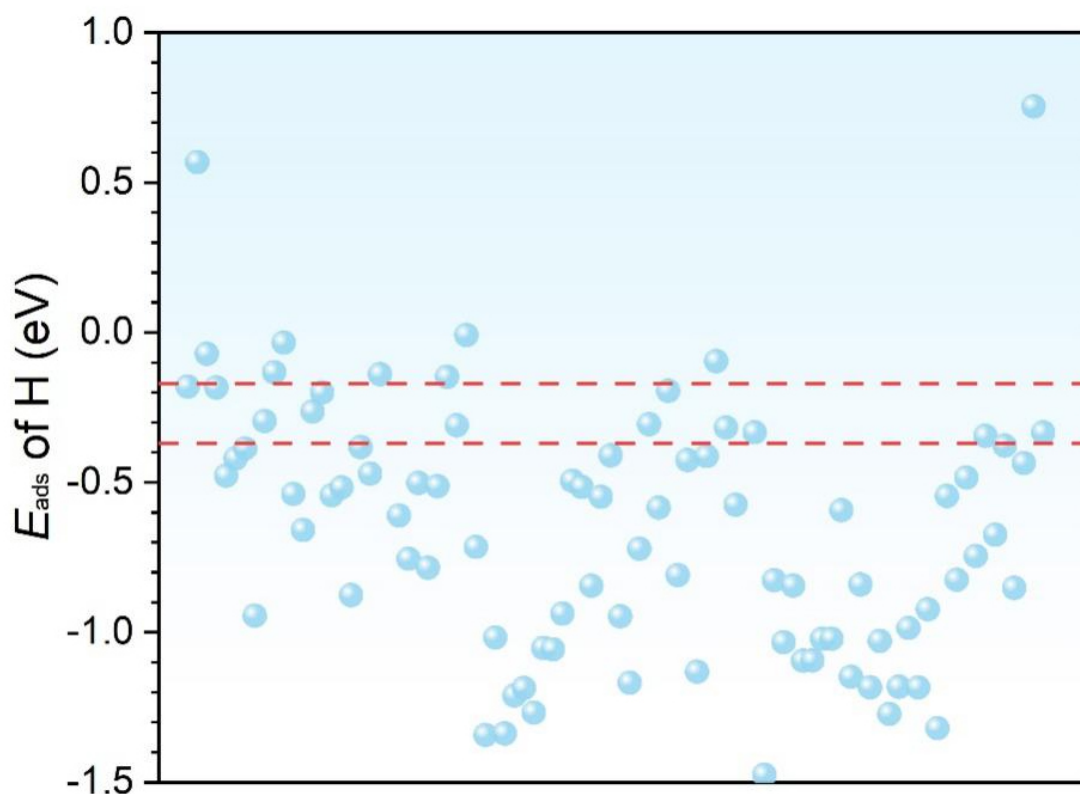


Figure 3. Adsorption energies of the most stable adsorption configurations of hydrogen atoms on different topological materials. The points in between the red dotted lines show those with E_{ads} of hydrogen within the -0.27 ± 0.1 eV. As reported in the literature, the adsorption energies close to -0.27 eV typically balance the hydrogen binding strength required for optimal HER activity^[31]. HER: Hydrogen evolution reaction.

Discussion

Experimental studies on topological materials have demonstrated favorable catalytic properties that align well with our predictions, particularly regarding adsorption energies and ΔG_{H^+} values. For example, Qu *et al.* reported that Bi_2Te_3 , a topological insulator, exhibited significant HER activity, achieving a current density of $1.74 \mu\text{A cm}^{-2}$, with partially oxidized surfaces contributing to enhanced catalysis^[22]. Boukhvalov *et al.* demonstrated the HER activity of the topological nodal-line semimetal AuSn_4 , attributing its performance to unique surface states that facilitated electron transfer^[24]. These findings highlight that topological materials can possess intrinsically advantageous properties for HER, supporting our predictions regarding adsorption sites and ΔG_{H^+} in the materials we studied.

In the present study, we selected an adsorption energy range of -0.27 ± 0.1 eV to evaluate HER performance. This criterion is based on previous studies that adsorption energies close to -0.27 eV typically balance the hydrogen binding strength required for optimal HER activity^[31,33]. By adopting this criterion, our study provides a robust approach that can be replicated and built upon in future HER research involving topological materials.

Our study relies on the ΔG_{H^+} as a primary descriptor for assessing HER activity. While ΔG_{H^+} has been widely used as an adequate descriptor for evaluating HER performance, it may not fully capture the complex mechanisms of catalytic performance, especially in topological materials, where unique surface states and electronic properties are integral to their functionality^[36]. In topological materials, the presence of surface states and high electron mobility could affect HER performance by facilitating charge transfer, enhancing

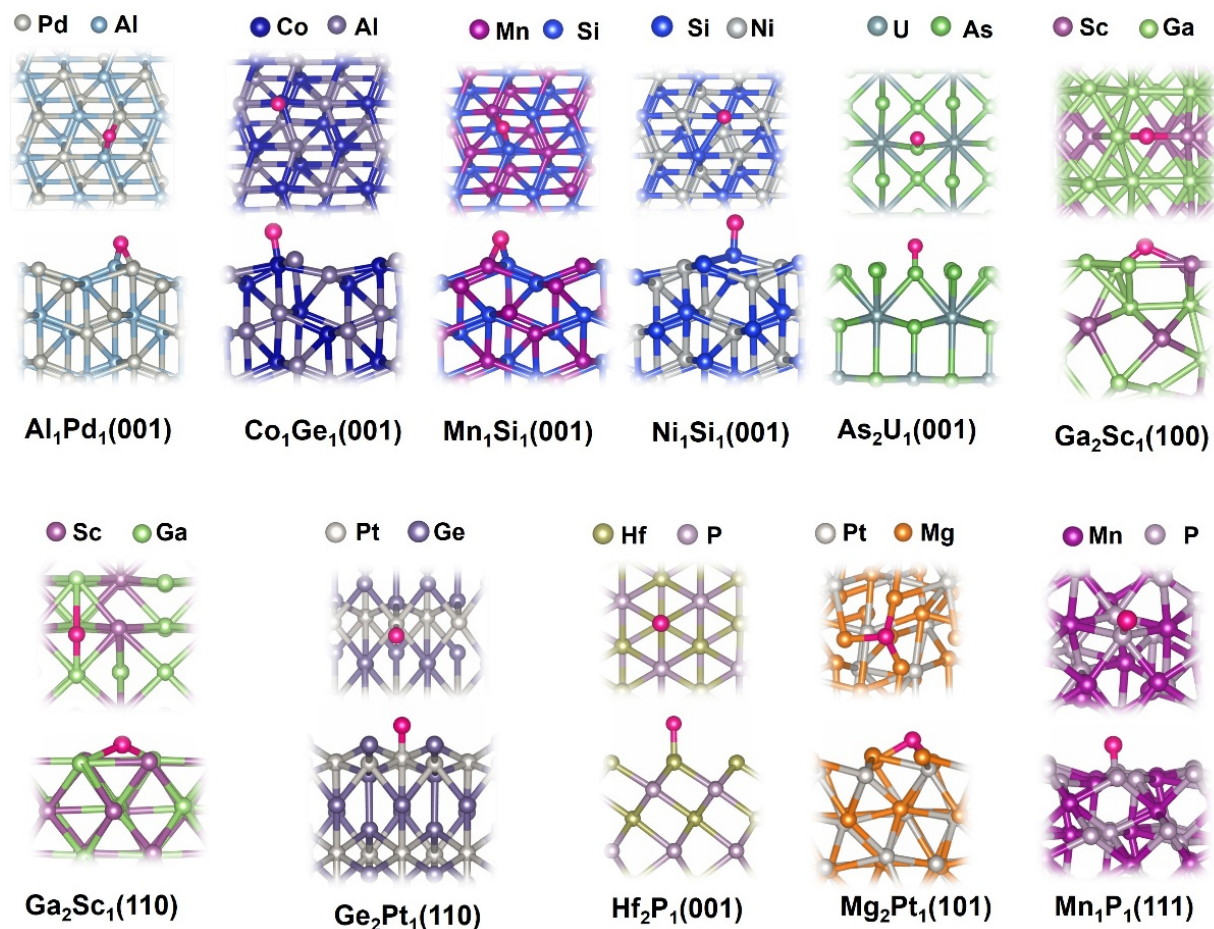


Figure 4. Top views and side views of the most stable hydrogen adsorption sites on 11 promising topological materials. The pink spheres represent hydrogen atoms, and the color schemes for other atoms are also provided for each topological material.

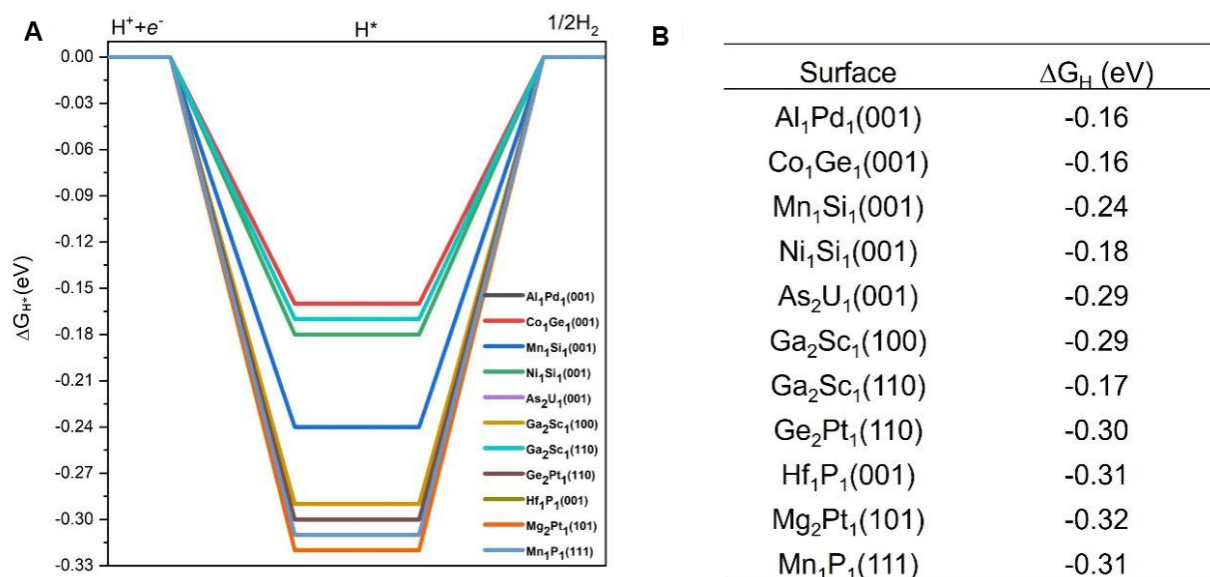


Figure 5. (A) DFT calculated free energy diagrams for HER on the 11 promising topological quantum materials with their corresponding surface termination. These eleven candidates are identified based on their optimal hydrogen adsorption energies, as discussed in Section 3.3. Some curves overlap due to similar ΔG_H values among different materials and surface terminations; (B) Summary table listing the corresponding adsorption surfaces and their calculated ΔG_H values. A ΔG_H value close to 0 eV is regarded as optimal for effective HER catalytic activity. HER: Hydrogen evolution reaction; DFT: density functional theory; ΔG_H : Gibbs free energy of hydrogen adsorption.

catalytic activity even if ΔG_{H^+} values are suboptimal. Furthermore, reaction kinetics, including hydrogen diffusion rates on the catalyst surface, are essential for understanding HER mechanisms and can vary significantly in materials with complex electronic structures. In the future, electronic structure calculations, such as projected density of states (DOS) and Bader charge analysis, may be incorporated to further elucidate the charge transfer characteristics and reaction kinetics of the selected topological materials.

The DOS of 11 representative high-performance HER catalysts were calculated, and the corresponding d-band and p-band centers were extracted [Supplementary Figure 1]. Unlike conventional transition-metal catalysts, these topological materials do not exhibit a clear correlation between traditional electronic descriptors and HER performance. This deviation is likely attributed to the unique electronic characteristics of topological materials, such as nontrivial band topology, gapless surface states and surface Fermi arc states^[36,37]. Clearly, a more in-depth exploration of unconventional electronic descriptors and their quantitative correlations with catalytic activity in these systems represents a fascinating direction for future research.

CONCLUSIONS

We conducted a comprehensive computational investigation of nearly 100 surfaces of topological materials to identify high-performance topological catalysts for efficient HER. We examined over 1,000 adsorption sites, including top, bridge, and various multi-fold sites. Our findings reveal that these topological materials exhibit a broad range of hydrogen adsorption energies, primarily ranging from -1.5 eV to 0 eV. Since previous studies suggested an optimal adsorption energy of -0.27 eV for ideal HER performance, we focused on materials with adsorption energies within -0.27 ± 0.1 eV. The computed Gibbs free energy ΔG_{H^+} values for these materials in the HER range from -0.31 eV to -0.16 eV, and detailed configurations for hydrogen adsorptions are provided. Ultimately, we identified 11 topological materials as promising catalysts for superior HER catalytic activity. Among these 11 topological materials, four candidates have ΔG_{H^+} very close to zero [$\text{Al}_1\text{Pd}_1(001)$, $\text{Co}_1\text{Ge}_1(001)$, $\text{Ni}_1\text{Si}_1(001)$ and $\text{Ga}_2\text{Sc}_1(110)$ with ΔG_{H^+} of -0.16, -0.16, -0.18 and -0.17 eV, respectively], indicating that they are likely to achieve the highest HER performance. These findings establish that topological materials possess abundant and diverse active sites, resulting in a wide range of hydrogen adsorption energies, thus enabling promising HER performance. These results can serve as a reliable dataset for further machine-learning studies and also offer valuable insights and guidelines for further theoretical and experimental exploration of topological materials as high-performance HER catalysts.

DECLARATIONS

Acknowledgments

The authors gratefully acknowledge the use of computing resources at the Agency for Science, Technology and Research (A*STAR) Computational Centre and the National Supercomputer Centre, Singapore.

Authors' contributions

DFT calculations, formal analysis, writing, and review: Yang, J.
Formal analysis, review, and editing: Wu, Y.; Yu, Z.
Discussion and review: Politano, A.; Bukhvalov, D.; Cupolillo, A.
DFT calculations, formal analysis, and supervision: Feng, H.
Conceptualization and supervision: Zhang, X.; Zhang, Y. W.

Availability of data and materials

The raw data supporting the conclusions of this article are available from the authors upon reasonable request.

AI and AI-assisted tools statement

Not applicable.

Financial support and sponsorship

This work was supported by the Italy-Singapore Science and Technology Cooperation (Grant No. R23101R040), the Singapore A*STAR SERC CRF Award, and the National Natural Science Foundation of China (22473007). Work at the University of L'Aquila and Calabria was funded by the European Commission - Next Generation EU, Mission 4 Component C2, Investment 1.1, under the Ministry of University and Research (MUR) of Italy PRIN 2022 (CUP: E53D23001750006, Grant No. 2022LFWJBR, acronym PLANET) and PRIN PNRR (CUP: E53D23018280001, Grant No. P20223LXTA, acronym ENTANGLE) projects. Politano, A.; Cupolillo, A.; Zhang, Y. W. acknowledge the EURIPIDES project, funded within the framework of the Italy-Singapore Science and Technology Cooperation 2023-2025 (Grant No. R23101R040 for A*STAR in Singapore and SG23GR07 for the Italian MAECI, Ministry of Foreign Affairs and International Cooperation).

Conflicts of interest

All authors declared that there are no conflicts of interest.

Ethical approval and consent to participate

Not applicable.

Consent for publication

Not applicable.

Copyright

© The Author(s) 2026.

Supplementary Materials

[Supplementary Materials](#)

REFERENCES

1. Beasy, K.; Ajulo, O.; Emery, S.; Lodewyckx, S.; Lloyd, C.; Islam, A. Advancing a hydrogen economy in Australia: public perceptions and aspirations. *Int. J. Hydrogen. Energy.* **2024**, *55*, 199-207. [DOI](#)
2. Koneczna, R.; Cader, J. Towards effective monitoring of hydrogen economy development: a European perspective. *Int. J. Hydrogen. Energy.* **2024**, *59*, 430-46. [DOI](#)
3. Hassan, A.; Ilyas, S. Z.; Jalil, A.; Ullah, Z. Monetization of the environmental damage caused by fossil fuels. *Environ. Sci. Pollut. Res. Int.* **2021**, *28*, 21204-11. [DOI PubMed](#)
4. Tiedje, J. M.; Bruns, M. A.; Casadevall, A.; et al. Microbes and climate change: a research prospectus for the future. *mBio* **2022**, *13*, e0080022. [DOI PubMed PMC](#)
5. San-Akca, B.; Sever, S. D.; Yilmaz, S. Does natural gas fuel civil war? Rethinking energy security, international relations, and fossil-fuel conflict. *Energy. Res. Soc. Sci.* **2020**, *70*, 101690. [DOI PubMed PMC](#)
6. Züttel, A.; Remhof, A.; Borgschulte, A.; Friedrichs, O. Hydrogen: the future energy carrier. *Philos. Transact. A. Math. Phys. Eng. Sci.* **2010**, *368*, 3329-42. [DOI PubMed](#)
7. Kazemi, A.; Manteghi, F.; Tehrani, Z. Metal Electrocatalysts for hydrogen production in water splitting. *ACS. Omega.* **2024**, *9*, 7310-35. [DOI PubMed PMC](#)
8. Alasali, F.; Abuashour, M. I.; Hammad, W.; Almomani, D.; Obeidat, A. M.; Holderbaum, W. A review of hydrogen production and storage materials for efficient integrated hydrogen energy systems. *Energy. Sci. Eng.* **2024**, *12*, 1934-68. [DOI](#)
9. Mei, L.; Zhang, Y.; Ying, T.; et al. Photochemical reduction of ultrasmall Pt nanoparticles on single-layer transition-metal dichalcogenides for hydrogen evolution reactions. *Mater. Today. Energy.* **2024**, *42*, 101487. [DOI](#)
10. Chen, J.; Aliasgar, M.; Zamudio, F. B.; et al. Diversity of platinum-sites at platinum/fullerene interface accelerates alkaline hydrogen evolution. *Nat. Commun.* **2023**, *14*, 1711. [DOI PubMed PMC](#)
11. Smiljanić, M.; Panić, S.; Bele, M.; et al. Improving the HER Activity and stability of Pt nanoparticles by titanium oxynitride support. *ACS. Catal.* **2022**, *12*, 13021-33. [DOI PubMed PMC](#)
12. Peng, X.; Jin, X.; Gao, B.; Liu, Z.; Chu, P. K. Strategies to improve cobalt-based electrocatalysts for electrochemical water splitting. *J. Catal.* **2021**, *398*, 54-66. [DOI](#)

-
13. Fang, W.; Wu, Y.; Xin, S.; et al. Fe and Mo dual-site single-atom catalysts for high-efficiency wide-pH hydrogen evolution and alkaline overall water splitting. *Chem. Eng. J.* **2023**, *468*, 143605. DOI
 14. Huo, L.; Jin, C.; Jiang, K.; Bao, Q.; Hu, Z.; Chu, J. Applications of nickel-based electrocatalysts for hydrogen evolution reaction. *Adv. Energy. Sustain. Res.* **2022**, *3*, 2100189. DOI
 15. Shao, W.; Xing, Z.; Xu, X.; et al. Bioinspired proton pump on ferroelectric HfO₂-coupled Ir catalysts with bidirectional hydrogen spillover for pH-universal and superior hydrogen production. *J. Am. Chem. Soc.* **2024**, *146*, 27486-98. DOI
 16. Yang, J.; Yu, Z. G.; Zhang, Y. W. Synergizing Cu dimers and N atoms in graphene towards an active catalyst for hydrogen evolution reaction. *Nanoscale. Adv.* **2021**, *3*, 5332-8. DOI PubMed PMC
 17. Zheng, Y.; Xiao, S.; Xing, Z.; et al. Oxophilic vanadium and deprotonated ruthenium atoms on tungsten carbide with accelerated intermediate migration for high-performance seawater hydrogen evolution. *Nano. Energy.* **2024**, *127*, 109769. DOI
 18. Zheng, Y.; Geng, W.; Xiao, S.; et al. Interfacial Ir-V direct metal bonding enhanced hydrogen evolution activity in vanadium oxides supported catalysts. *Angew. Chem. Int. Ed.* **2024**, *63*, e202406427. DOI
 19. Keimer, B.; Moore, J. E. The physics of quantum materials. *Nat. Phys.* **2017**, *13*, 1045-55. DOI
 20. Kumar, N.; Guin, S. N.; Manna, K.; Shekhar, C.; Felser, C. Topological quantum materials from the viewpoint of chemistry. *Chem. Rev.* **2021**, *121*, 2780-815. DOI PubMed PMC
 21. Luo, H.; Yu, P.; Li, G.; Yan, K. Topological quantum materials for energy conversion and storage. *Nat. Rev. Phys.* **2022**, *4*, 611-24. DOI
 22. Qu, Q.; Liu, B.; Liang, J.; et al. Expediting hydrogen evolution through topological surface states on Bi₂Te₃. *ACS. Catal.* **2020**, *10*, 2656-66. DOI
 23. Li, J.; Ma, H.; Xie, Q.; et al. Topological quantum catalyst: dirac nodal line states and a potential electrocatalyst of hydrogen evolution in the TiSi family. *Sci. China. Mater.* **2017**, *61*, 23-9. DOI
 24. Boukhvalov, D. W.; D'Olimpio, G.; Mazzola, F.; et al. Unveiling the catalytic potential of topological nodal-line semimetal AuSn₄ for hydrogen evolution and CO₂ reduction. *J. Phys. Chem. Lett.* **2023**, *14*, 3069-76. DOI
 25. Kresse, G.; Furthmüller, J. Efficient iterative schemes for ab initio total-energy calculations using a plane-wave basis set. *Phys. Rev. B.* **1996**, *54*, 11169. DOI
 26. Kresse, G.; Hafner, J. Ab initio molecular-dynamics simulation of the liquid-metal-amorphous-semiconductor transition in germanium. *Phys. Rev. B.* **1994**, *49*, 14251. DOI
 27. Perdew, J. P.; Burke, K.; Ernzerhof, M. Generalized gradient approximation made simple. *Phys. Rev. Lett.* **1996**, *77*, 3865-8. DOI PubMed PMC
 28. Blöchl, P. E. Projector augmented-wave method. *Phys. Rev. B.* **1994**, *50*, 17953. DOI PubMed
 29. Kresse, G.; Joubert, D. From ultrasoft pseudopotentials to the projector augmented-wave method. *Phys. Rev. B.* **1999**, *59*, 1758-75. DOI PMC
 30. Petrilli, H. M.; Blöchl, P. E.; Blaha, P.; Schwarz, K. Electric-field-gradient calculations using the projector augmented wave method. *Phys. Rev. B.* **1998**, *57*, 14690-7. DOI
 31. Grimme, S.; Antony, J.; Ehrlich, S.; Krieg, H. A consistent and accurate ab initio parametrization of density functional dispersion correction (DFT-D) for the 94 elements H-Pu. *J. Chem. Phys.* **2010**, *132*, 154104. DOI
 32. Nørskov, J. K.; Bligaard, T.; Logadottir, A.; et al. Trends in the exchange current for hydrogen evolution. *J. Electrochem. Soc.* **2005**, *152*, J23. DOI
 33. Rothenberg, G. *Catalysis: concepts and green applications*; Wiley, 2008. DOI
 34. Greeley, J.; Jaramillo, T. F.; Bonde, J.; Chorkendorff, I. B.; Nørskov, J. K. Computational high-throughput screening of electrocatalytic materials for hydrogen evolution. *Nat. Mater.* **2006**, *5*, 909-13. DOI PubMed
 35. Liu, X.; Xiao, J.; Peng, H.; Hong, X.; Chan, K.; Nørskov, J. K. Understanding trends in electrochemical carbon dioxide reduction rates. *Nat. Commun.* **2017**, *8*, 15438. DOI PubMed PMC
 36. Meng, W.; Zhang, X.; Liu, Y.; et al. Multifold fermions and fermi arcs boosted catalysis in nanoporous electride 12CaO-7Al₂O₃. *Adv. Sci.* **2023**, *10*, e2205940. DOI PubMed PMC
 37. Li, M.; Zhang, X.; Chen, C.; Kou, L. Topological catalysis driven by symmetry-protected surface states. *Nano. Lett.* **2026**, *26*, 887-93. DOI PubMed

Disclaimer/Publisher's Note: All statements, opinions, and data contained in this publication are solely those of the individual author(s) and contributor(s) and do not necessarily reflect those of OAE and/or the editor(s). OAE and/or the editor(s) disclaim any responsibility for harm to persons or property resulting from the use of any ideas, methods, instructions, or products mentioned in the content.



© The Author(s) 2026. Open Access This article is licensed under a Creative Commons Attribution 4.0 International License (<https://creativecommons.org/licenses/by/4.0/>), which permits unrestricted use, sharing, adaptation, distribution and reproduction in any medium or format, for any purpose, even commercially, as long as you give appropriate credit to the original author(s) and the source, provide a link to the Creative Commons license, and indicate if changes were made.